FLAG

Seismic Images Beneath the Bottomless Pits (Continental) Area of Flagstaff, Arizona

Submitted By

R.D. Catchings, M.N. Jaasma, M.R. Goldman, and M.J. Rymer
U.S. Geological Survey

PASSCAL Data Report 98-002
Report 1 of 2

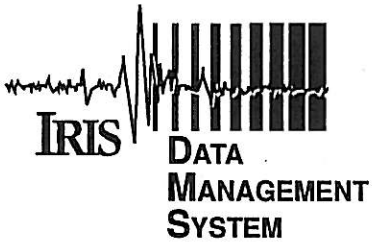

Distributed by

Incorporated Research Institutions for Seismology
Data Management Center
1408 NE 45th Street
Suite 201
Seattle, Washington 98105

Seismic Images Beneath The Bottomless Pits (Continental) Area of Flagstaff, Arizona

R. D. Catchings, M. N. Jaasma, M. R. Goldman, and M. J. Rymer
U. S. Geological Survey
345 Middlefield Rd. MS 977
Menlo Park, CA 94025

1997

Open-File Report 97-76

Table of Contents

List of Figures

List of Tables

Introduction

Water supplies for the City of Flagstaff, Arizona are derived from the Northern Arizona regional aquifer using deep wells. In the Flagstaff area, the regional aquifer occurs within the Coconino Sandstone and/or Supai Group at depths between about 900 ft and 1600 ft below ground surface (bgs) (Don Bills, pers. comm., 1995). Due to low permeability of the aquifer rocks, many water wells previously sited by the City of Flagstaff do not yield enough water to justify the appreciable cost of drilling.

Study of the existing water wells in the Flagstaff area shows that the most productive wells occur where permeability has been increased by significant faulting and fracturing of subsurface rocks. In 1994, at the request of the City of Flagstaff, scientists from the U.S. Geological Survey (USGS) began a program of geologic mapping to locate areas that have a high density of faults and/or fractures at the surface (Gary Mann, pers. comm., 1995). Three of the highest priority areas were identified by the City of Flagstaff in eastern and southern Flagstaff. In this report, we refer to those areas as: (1) the Bottomless Pits (Continental) area, (2) Skunk Canyon, and (3) Fox Glen (Figure 1A and 1B). This report focuses on the Bottomless Pits area. A separate report for Skunk Canyon and Fox Glen is given by Jaasma et al. (1997).

Because each of these preferred sites lies within an alluvial basin, the location of faulting or complexity of faulting was not known from surface mapping. Furthermore, at sites with significant surface faulting, the locations of highly fractured and faulted rocks are generally different at the surface than at the depths of the regional aquifer (Figure 2). For these reasons, the U.S. Geological Survey acquired seismic reflection and refraction data during October, 1995 and July, 1996 at each of the high-priority sites identified by the City of Flagstaff. In August and September, 1996, City of Flagstaff engineers located wells, in part, on the basis of fault and fracture patterns imaged in the seismic sections. At the time of the writing of this report, wells are being drilled at each of the sites. Preliminary indications are that the rocks are highly fractured at the depths of the regional aquifer in a manner similar to that imaged by the seismic techniques.

Geology of the Continental Area (Bottomless Pits)

The Bottomless Pits area, an alluvial flood plain surrounded by small (~30-50 m) fault-bounded hills (Figure 3), is located approximately 6 km east-northeast of downtown Flagstaff (Figure 1). Geologic mapping (Gary Mann, pers. comm., 1995) shows that the Continental area occurs at the intersection of two ~300-m-wide intersecting graben, a NW-SE-oriented graben and a NE-SW-oriented graben. At the western end of the NW-SE graben and near the intersection of the two graben is an opening to an apparent large-volume, underground cavern referred to as the "Bottomless Pits". Geologists in the

Seismic Images Beneath The Bottomless Pits (Continental) Area of Flagstaff, Arizona

R. D. Catchings, M. N. Jaasma, M. R. Goldman, and M. J. Rymer

1997

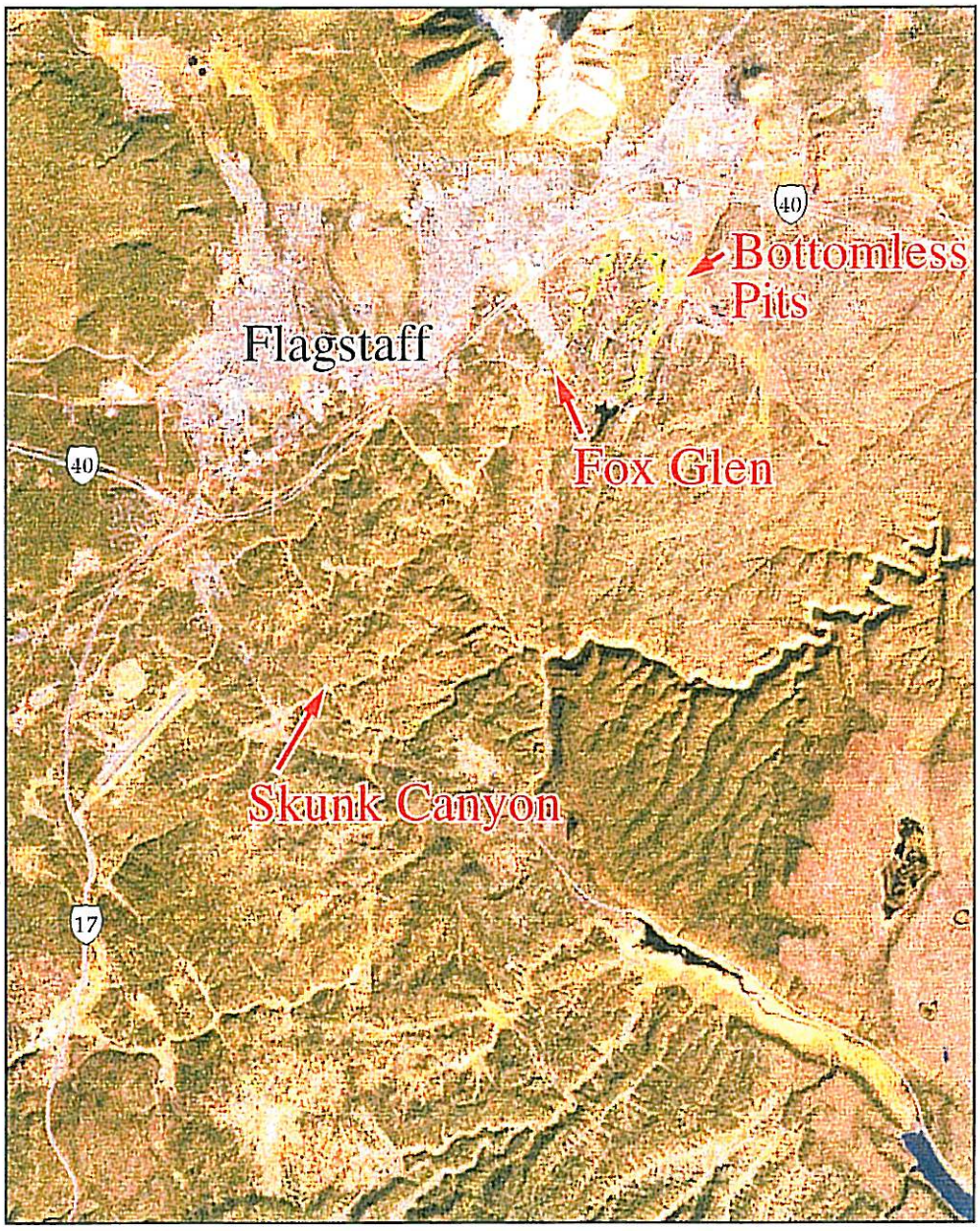

U. S. Geological Survey Open-File Report 97-76

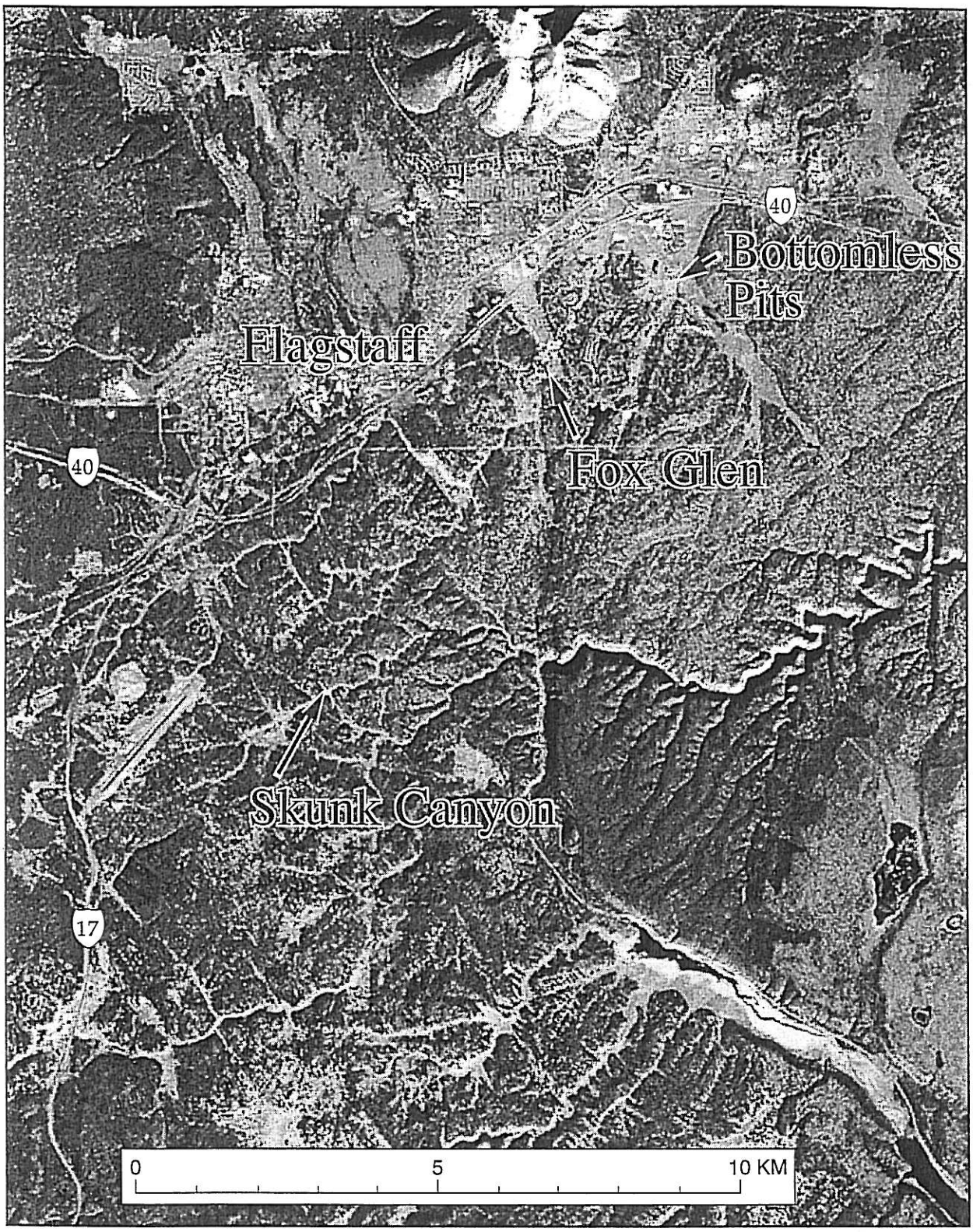

Figure 1A: Landsat satellite image of the Flagstaff, Arizona area with locations of study areas.

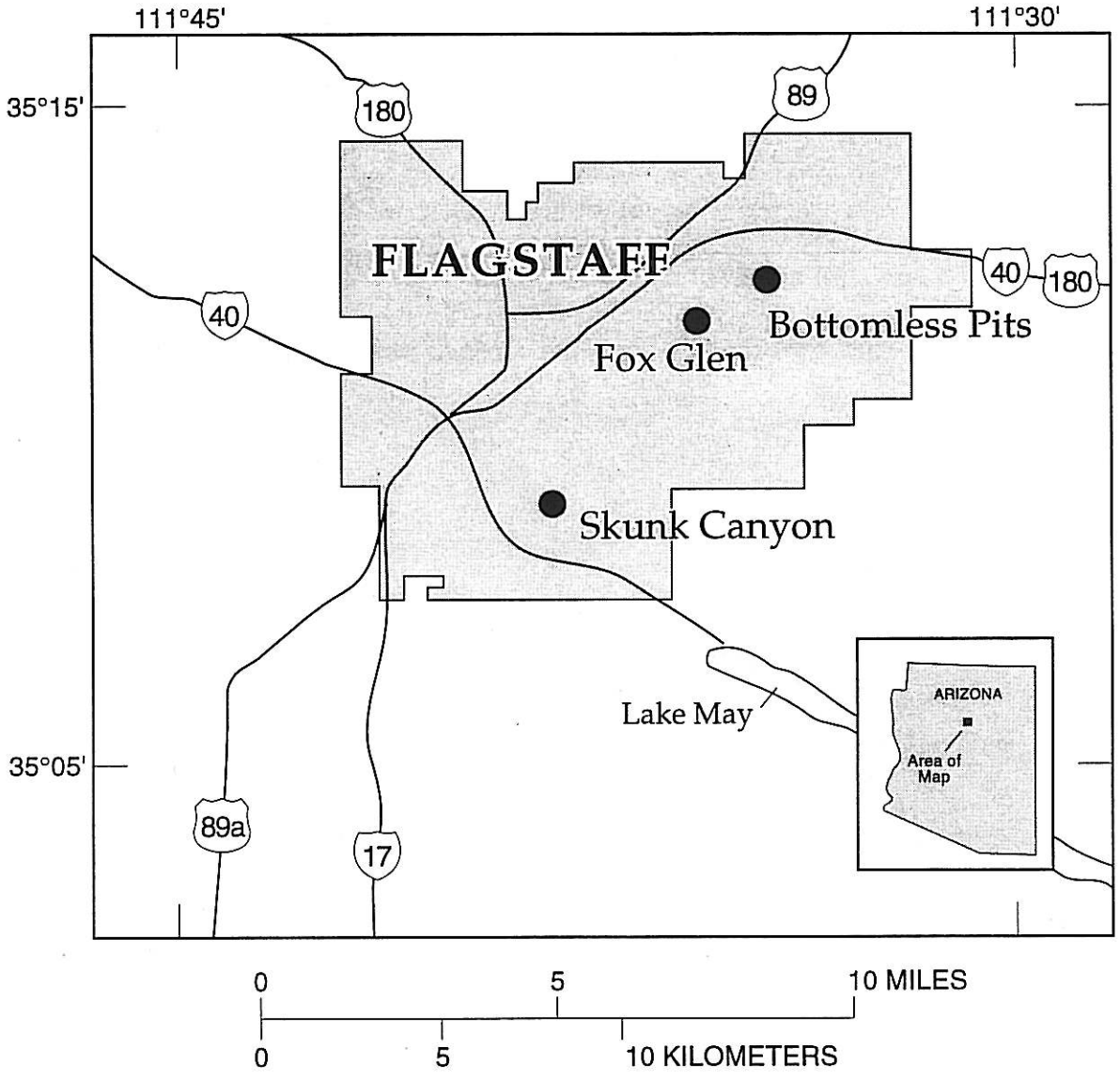

Figure 1B: Map of the Flagstaff, Arizona area and locations of study areas.

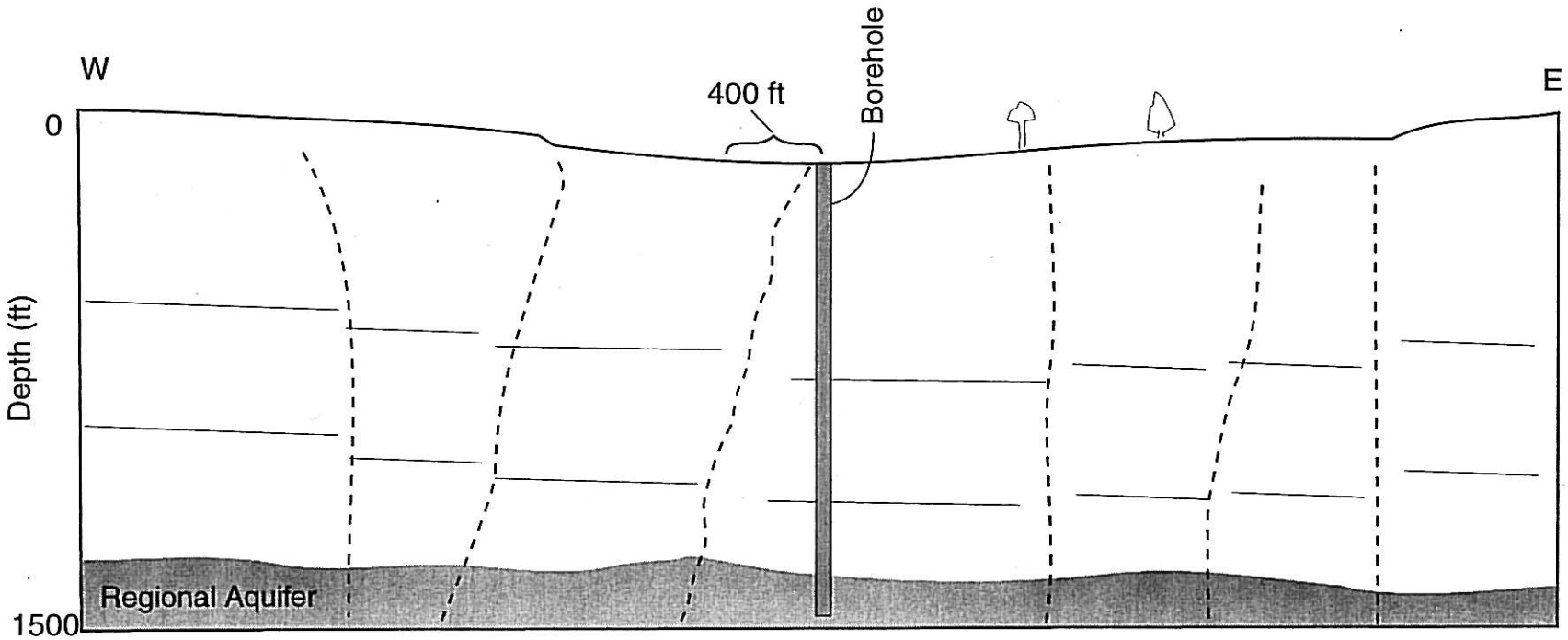

Figure 2: Hypothetical cross section depicting the effect of dipping faults/fractures in locating drill sites. If vertical wells are drilled into the surface locations of dipping faults, the well may not intersect the fractured part of the aquifer. For a fault/fracture system that dips 15 degrees from vertical, the fault/fracture system would intersect the regional aquifer 400 ft from its surface location.

USGS Flagstaff office report that the Bottomless Pits cavern can accomodate very large volumes of water for many hours during flood stages (Don Bills, pers. comm., 1995), suggesting that the cavern is extensive. The alluvial fill within the graben is generally less than a few meters thick and is underlain by flat-lying or gently dipping Kaibab Limestone. The alluvial thickness can be seen at the entrance to the Bottomless Pits, where the alluvium and Kaibab Limestone that forms the roof of the cavern are only a few meters thick. Kaibab Limestone can also be seen in exposures on the surrounding hills.

The Bottomless Pits area is considered an ideal target for water exploration because it is located within the flow direction of the regional aquifer, it occurs at the intersection of two graben - suggesting abundant faulting and fracturing at depth, it is known to accomodate large volumes of water during flood stages, and the depth to the regional aquifer in this area is estimated to be less than 1500 ft (~500 m) bgs.

Seismic Acquisition Techniques

Geologists and geophysicists from the U.S. Geological Survey employed several other geophysical techniques at the high-priority sites, including gravity measurements, ground-penetrating radar, and square-array resistivity, but due to the depths of the regional aquifer and the resolution needed, city of Flagstaff Officials also chose to use seismic-reflection techniques. We chose to simultaneously acquire seismic reflection and refraction data to minimize the cost and maximize our understanding of the subsurface. With narrow targets such as faults and fractures, vertical water wells would have to be sited within a few meters of the intersection of the fault/fracture system and the water table (Figure 2). Seismic reflection methods are the best of the available geophysical methods to achieve the required resolution at the depth of the regional aquifer. Seismic refraction data were used to gain better depth precision and to better estimate the composition of the subsurface rocks.

Seismic Survey

The USGS acquired seismic data along two perpendicular seismic profiles at the Bottomless Pits area (Figure 3). Line 1 originated within the NW-SE graben, crossed an ~40-m-high fault-line scarp, and ended on a nearly flat mesa. Line 2 was located within the NE-SW graben and crossed the intersection of the two graben. The opening to the large subsurface cavern (referred to as the "Bottomless Pits") is within a few tens of meters of the origin of Line 1.

The seismic data were acquired using explosive sources buried to depths of approximately 3 m (10 ft) and spaced approximately 5 m apart (Appendix 1 and 2). Shots were fired using electrical blasting caps that were detonated with a USGS-designed shooting system. We used Mark Products L-28 (28-Hz) sensors, spaced approximately every 2.5 m (Appendix 1 and 2) and recorded the seismic records on an Oyo DAS-1 seismograph system. The DAS-1 was configured as a 144-active-channel system with sensors connected by

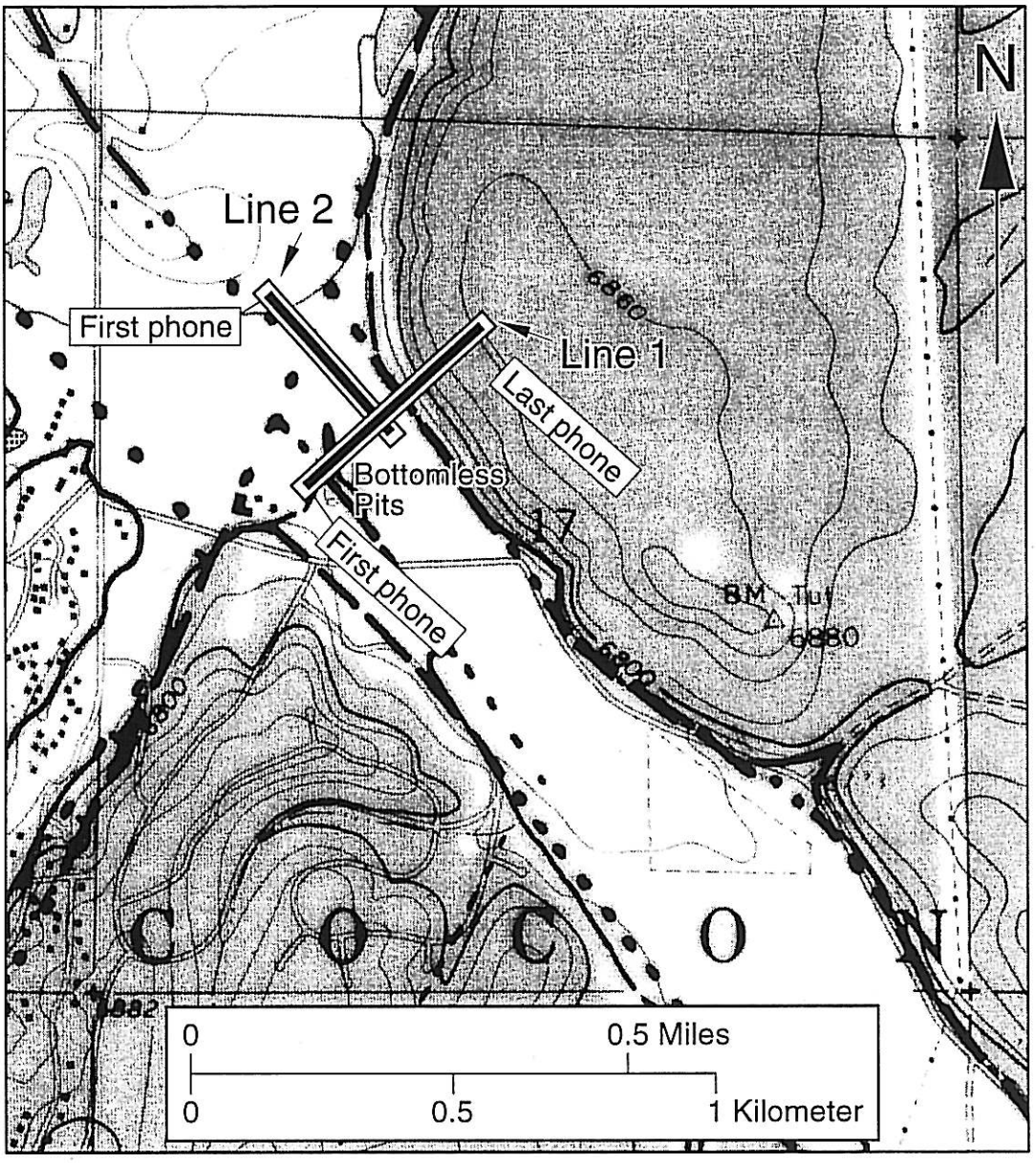

Figure 3: Topographic map of the Bottomless Pits area showing the location of seismic lines, mapped faults (dashed and dotted heavy black lines, from Gary Mann (pers. comm., 1995)), and cultural features. Elevations are in feet. The mapped faults suggest two intersecting grabens, one oriented NW-SE and the other NE-SW.

cable. Both the blaster and the seismograph were controlled by a synchronized timing clock that gave a 1-volt pulse at each minute. The 1-volt pulse triggered both the DAS-1 recording system and the blaster simultaneously. Shots were recorded as field files in chronological order, and acquisition parameters were recorded on each seismic record. We used 4-mm tapes to store the data in SEG-2 format for later retrieval and processing in the laboratory.

We used a "shoot-through" seismic survey in order to maximize fold near the centers of the profiles and to obtain tomographic-type velocity data. The total line length of Line 1 was 493.8 m, and Line 2 was 367.6 m (Table 1). A total of 60 shots were fired along Line 1, and 68 shots were fired along Line 2. Each shot was recorded for 5 seconds using a 0.5-ms sampling rate.

Table 1: Acquisition parameters for Line 1 and Line 2. Distances are relative to the first geophone of each of the recording arrays.

	Orientation	*Total Length (m)*	*Lenght of Shot Point Array (m)*	*# Shots*	*# CDP's*	*Max. Fold*
Line 1	*SW-NE*	*493.81*	*494.29*	*60*	*398*	*39*
Line 2	*NW-SE*	*367.56*	*365.14*	*68*	*293*	*64*

Locations

Line 1

Prior to data acquisition, shot and receiver locations were determined using a measuring tape and compass. Shot holes were then drilled using a 2-inch-diameter drill bit, and recording sites were determined. After the data were acquired, shot and sensor locations were more precisely determined using an electronic distance meter. The locations (distance and elevation) were measured to within 0.001 m (Appendix A and B).

Line 1 was acquired using two separate deployments of geophones. One hundred forty four geophones were deployed along the southwestern 360 m of the profile, and about 44 shots were fired into the array. The array was then deployed along the northeastern 360 m of the profile, and the remaining shots were fired into the array. There was approximately a 220-m overlap between the two recording arrays. A plot of geophone elevation variations along Line 1 is shown in Figure 4. Elevation is relative to the first geophone at the southwest end of the profile and varies by approximately 40 m along the profile. Due to siting errors prior to drilling shot holes and due to obstacles (trees, standing water, etc.), the recording array did not form a perfectly straight line; however, geophone locations varied from a straight line (connecting the endpoints) by not more than 5 m along the approximately 500-m-long profile (Figure 5).

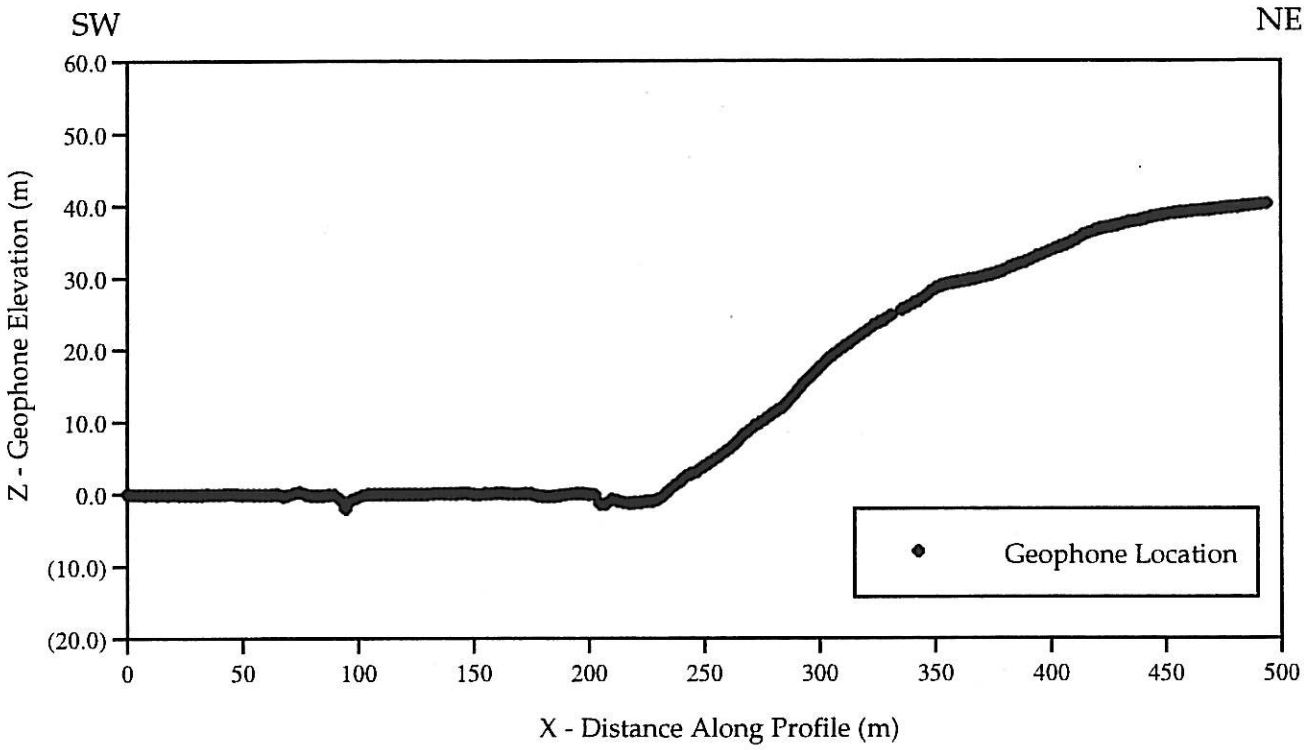

Figure 4: Relative geophone elevations (Line 1) as a function of distance along seismic line. Zero elevation is the elevation of the first geophone along Line 1.

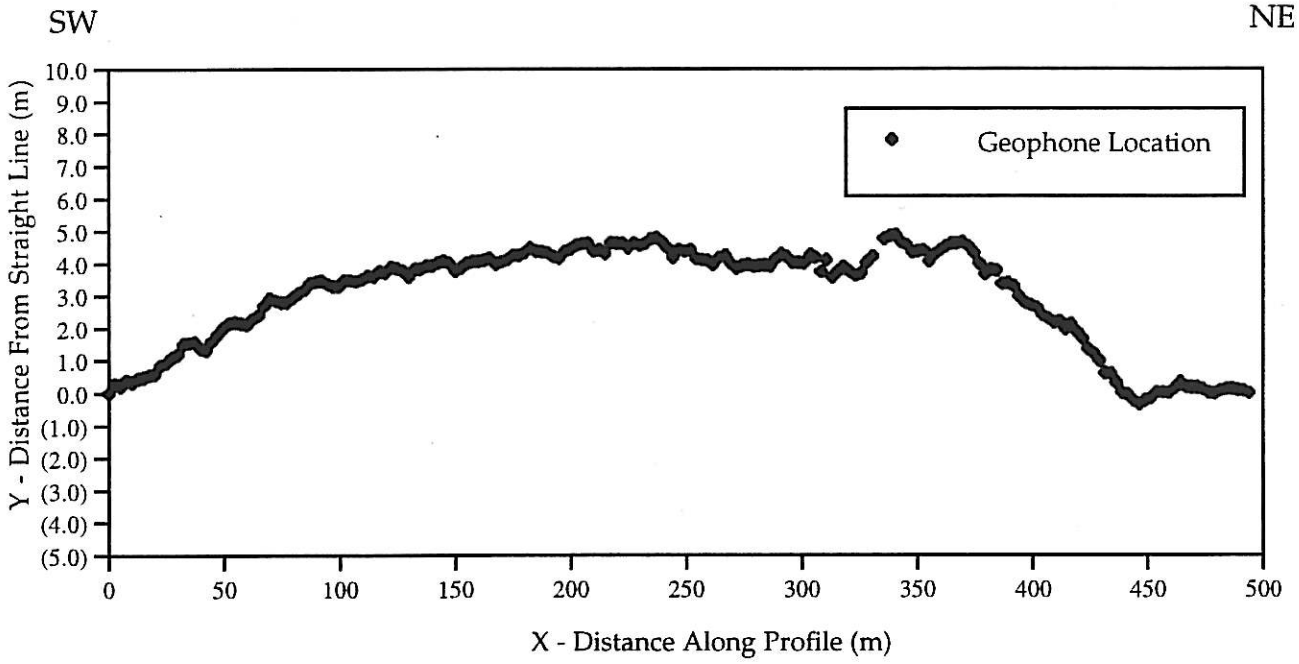

Figure 5: Geophone variation (Line 1) from a straight line connecting the first and last geophone.

Due to cultural features (pipelines, sewer lines, etc.), a steep ~40-m rise in elevation, and locally dense vegetation on the hill of Line 1, shot points could not be located along the entire line. Figure 6 shows shot point elevation as a function of distance along Line 1. There were no shot points located between approximately meter 232 and meter 440. Because shot points were located prior to making electronic measurements, the line of shot points also varied from a straight line. There was about a 5-m variance from a straight line along the ~500-m-long profile (Figure 7). We estimate that these variations in locations lead to an error in depth and location within the subsurface of less than about 2 m over the ~500-m-long profile.

Line 2

Because Line 2 was located within a graben, the elevation of the geophones varied by less than 2 m over the approximately 370 m of the seismic line (Figure 8). Due to siting errors prior to drilling shot holes, the recording array did not form a perfectly straight line; however, geophone locations varied from a straight line (connecting the endpoints) by not more than 3 m (Figure 9). Shot points were located along the length of Line 2, with the exception of a few shots that were skipped due to cultural features (Figure 10). Shot point locations varied from a straight line by less than 1.5 m along the 365-m-long profile (Figure 11). These minor variations in location have neglible effects on subsurface locations.

Data Processing

The seismic data were processed using a Promax processing system at our office in Menlo Park, CA. The following steps were involved in data processing:

- Geometry installation
- Trace editing
- Bandpass filtering
- Timing corrections
- Velocity analysis
- Moveout correction
- Velocity inversion
- Elevation statics
- Muting
- F-K filtering
- Stacking
- Migration

The locations determined from the electronic-distance-meter surveys were imported directly into the Promax processing routine. Due to poor coupling between the geophones and the earth, malfunctioning geophones,

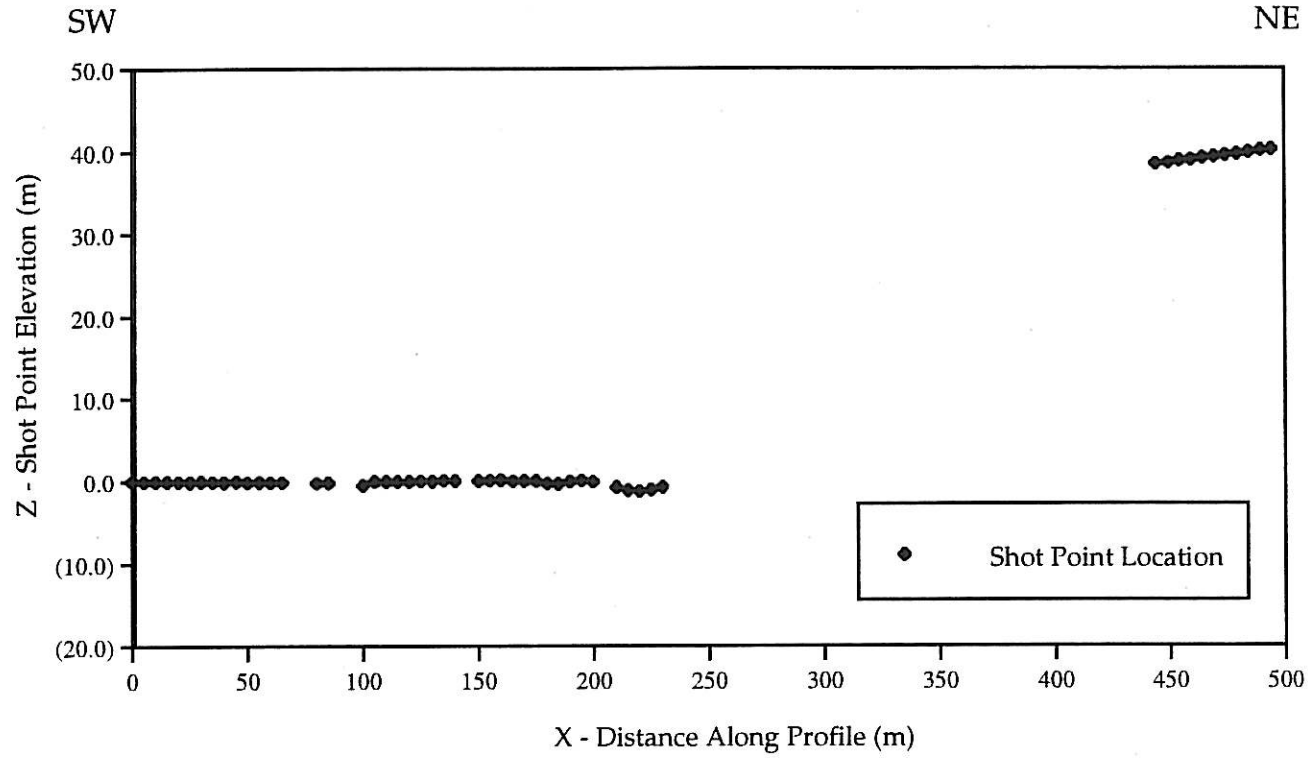

Figure 6: Relative shot point elevations (Line 1) as a function of distance along seismic line. Elevation is relative to the first shot point along Line 1.

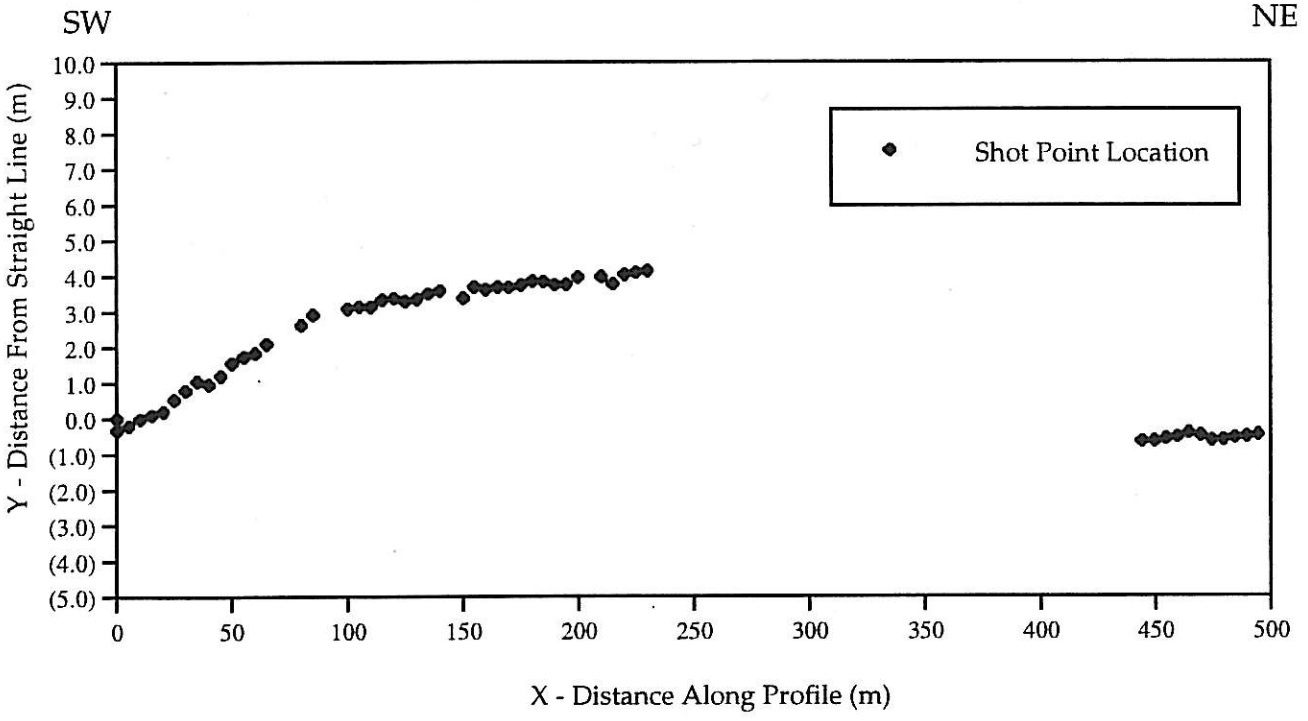

Figure 7: Shot point variation (Line 1) from a straight line connecting the first and last shot point.

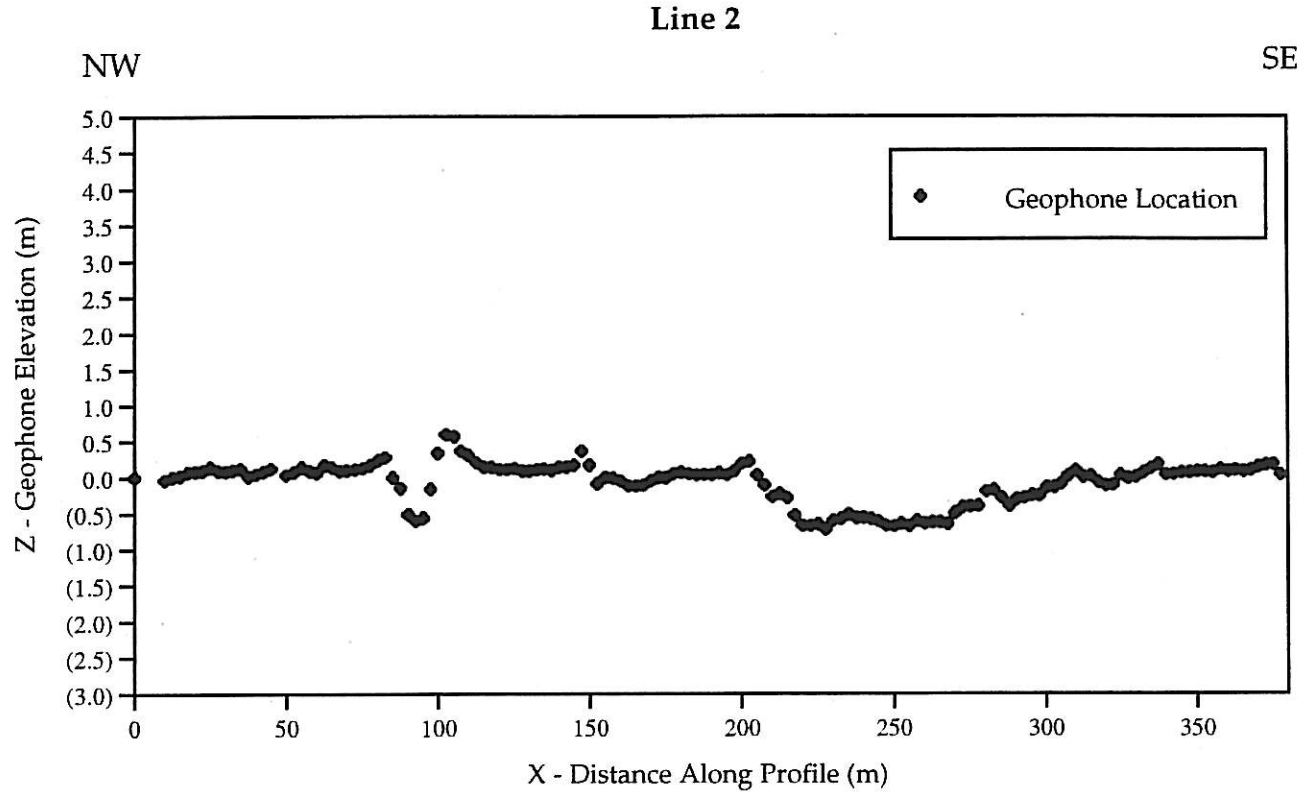

Figure 8: Relative geophone elevations (Line 2) as a function of distance along seismic line. Zero elevation is the elevation of the first geophone along Line 2.

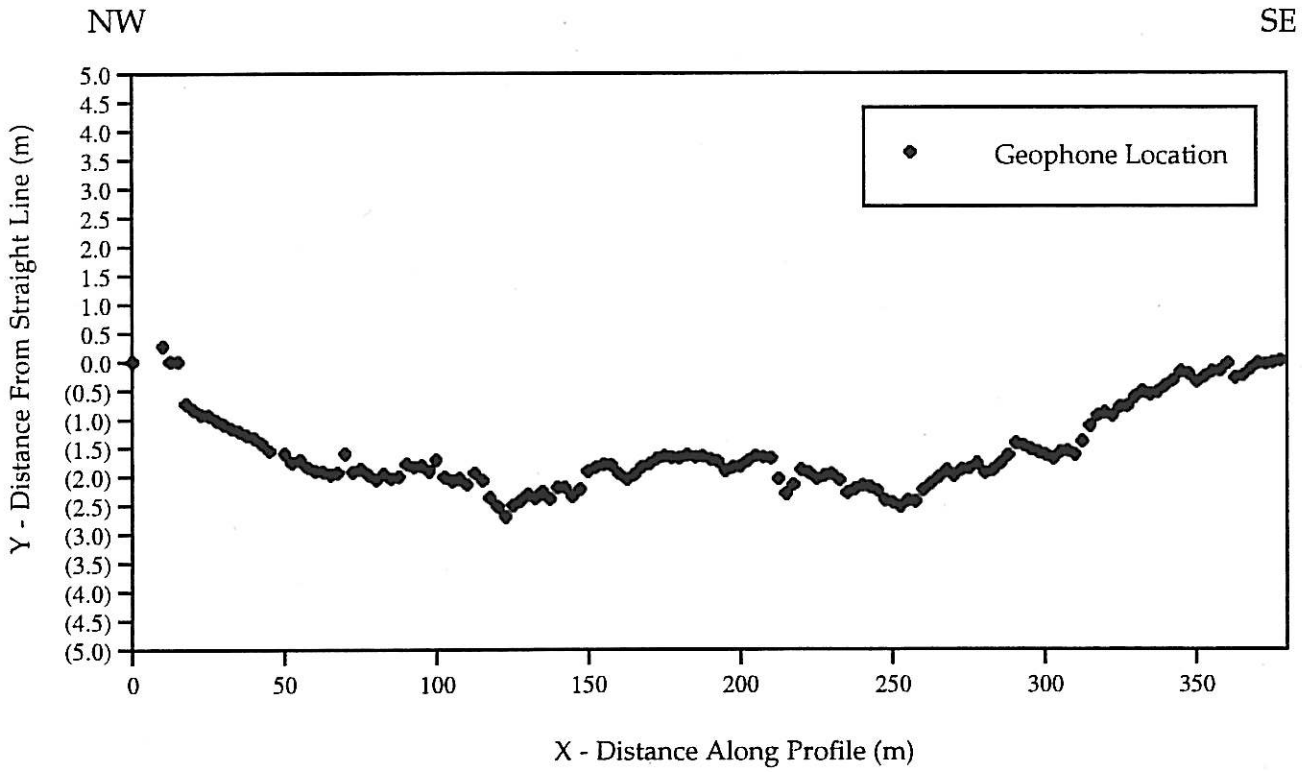

Figure 9: Geophone variation (Line 2) from a straight line connecting the first and last geophone.

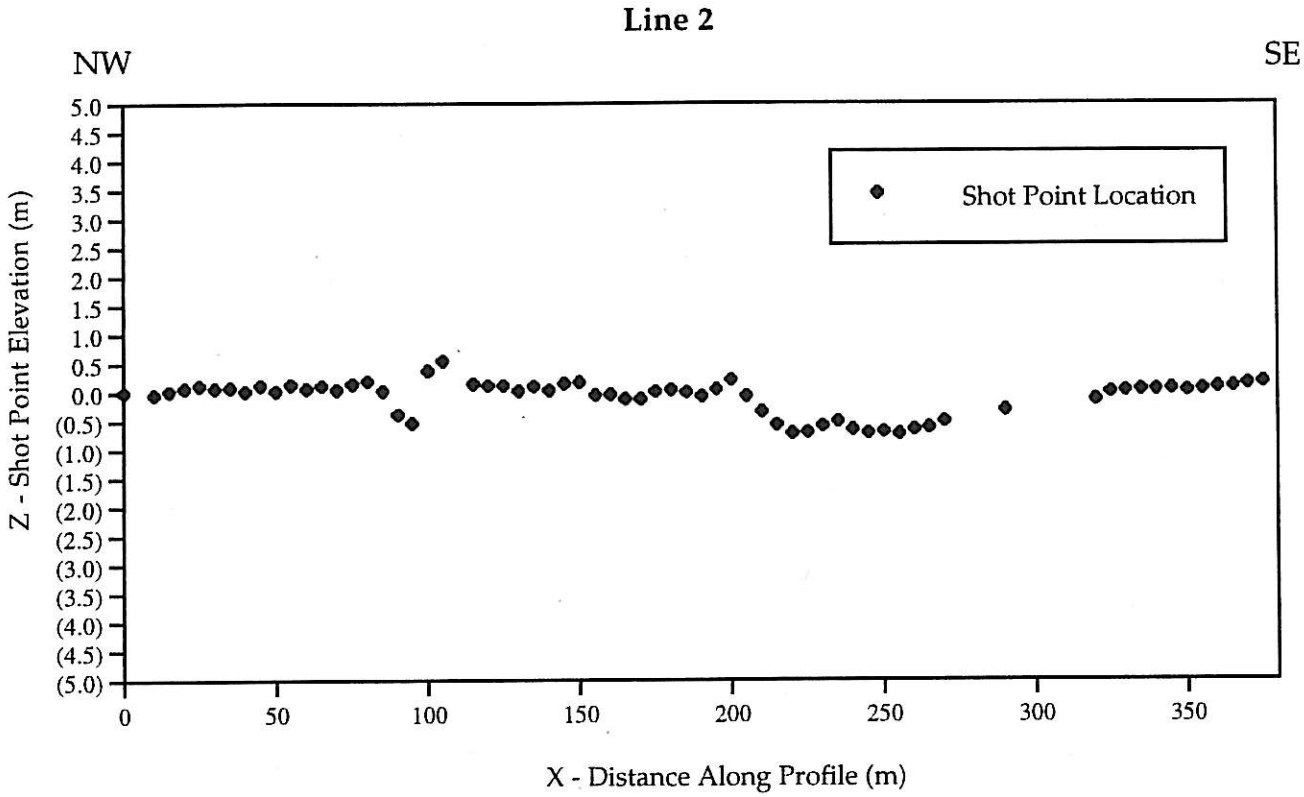

Figure 10: Relative shot point elevations (Line 2) as a function of distance along seismic line. Elevatior is relative to the first shot point along Line 2.

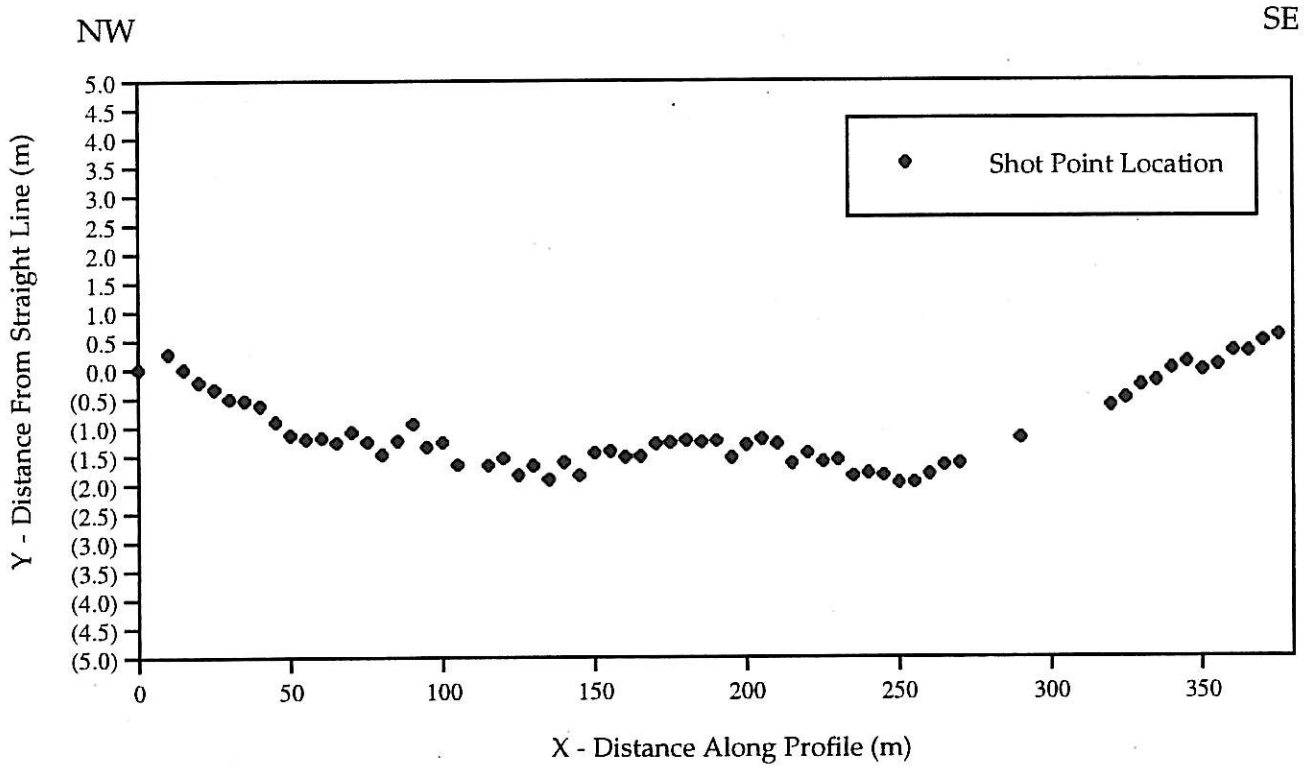

Figure 11: Shot point variation (Line 2) from a straight line connecting the first and last shot point.

and/or local noise sources along the seismic line, some unusually noisy traces had to be removed. The affected traces often varied from shot to shot; thus, separate trace edits were employed for each shot gather. We used bandpass filtering with a low cut of 30 Hz to remove most surface waves, shear waves, and cultural noise. A high cut of about 250 Hz was used to remove wind noises and other high-frequency noise.

Using the shoot-through acquisition method, the fold varied along the seismic profile (Figure 12). The fold for Line 1 also varied due to the shot point distribution and due to movement of the recording array. The maximum fold along Line 1 was approximately 38 for the first deployment and about 12 for the second deployment. Fold along Line 2 varied more systematically, whereby fold was one at the endpoints and a maximum of 65 near the center of the line (Figure 13).

Stacked Seismic Images

A stacked seismic section depicting the uppermost 600 m of the subsurface along Line 1 is shown in Figure 14. The elevation of the first recording geophone is used as the datum. Because we did not have shot points between meters 232 and 440, we did not image the shallow (<200 m) subsurface for that segment. The deeper subsurface (>200 m), however, is imaged because we undershot that area of the seismic line. Numerous faults were imaged along the seismic line, especially along the northeast half of the line. Line 1 originates on the southwest side of the graben near the underground cavern known as the Bottomless Pits. We suggest that similar underground caverns are imaged on the seismic section as blurred reverbative reflections (for example, see between CDP 125 and 150, CDP 50 to 100 and much of the area between CDP 0 and 50).

A stack of the first 600+ meters of Line 2 is shown in Figure 15. Elevation is relative to the first recording geophone on the northwest end of the profile. Numerous faults are shown along the profile, and there appears to be appreciable structural variation in the shallow subsurface.

Data Availability

The data presented in this report have been archived at the USGS (Menlo Park) and the IRIS-PASSCAL data center in SEG-Y format and are available as shot gathers with elevation and shot timing corrections applied. The Principal Investigators can be contacted at the address on the cover of this report for the digital data.

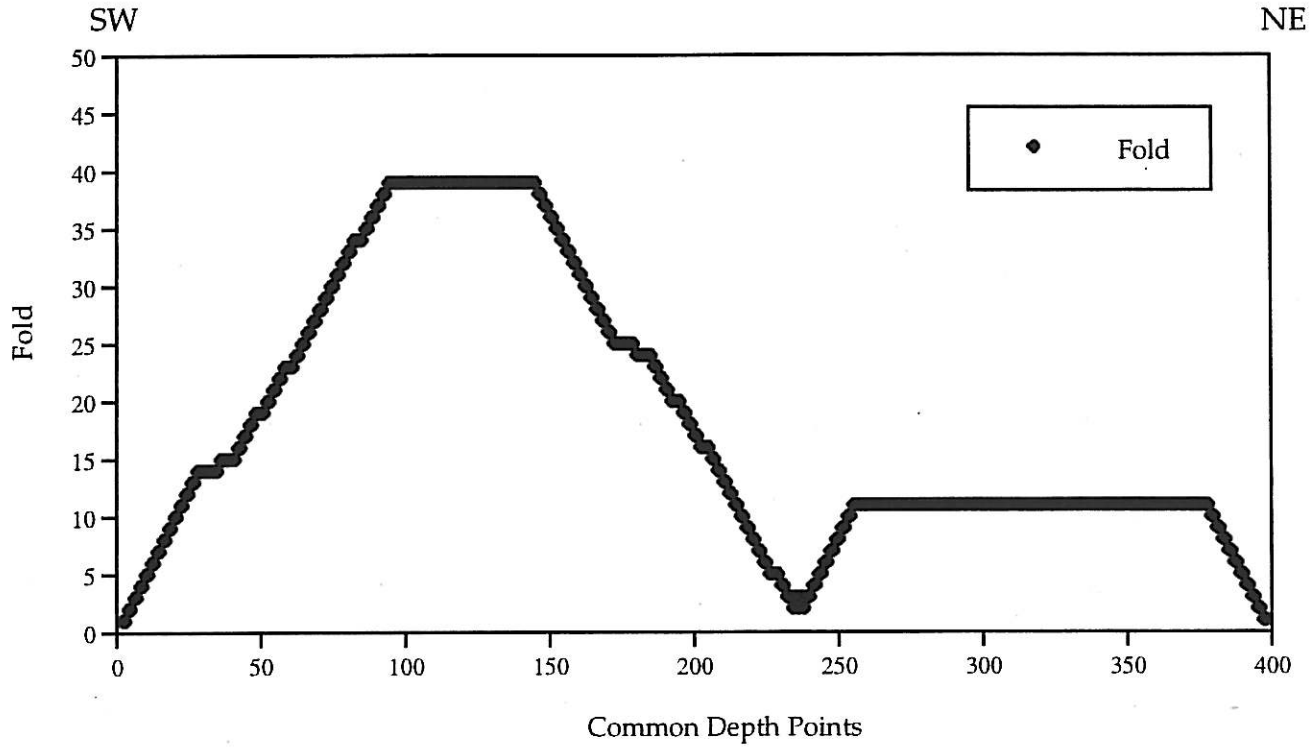

Figure 12: Fold as a function of common depth points (Line 1).

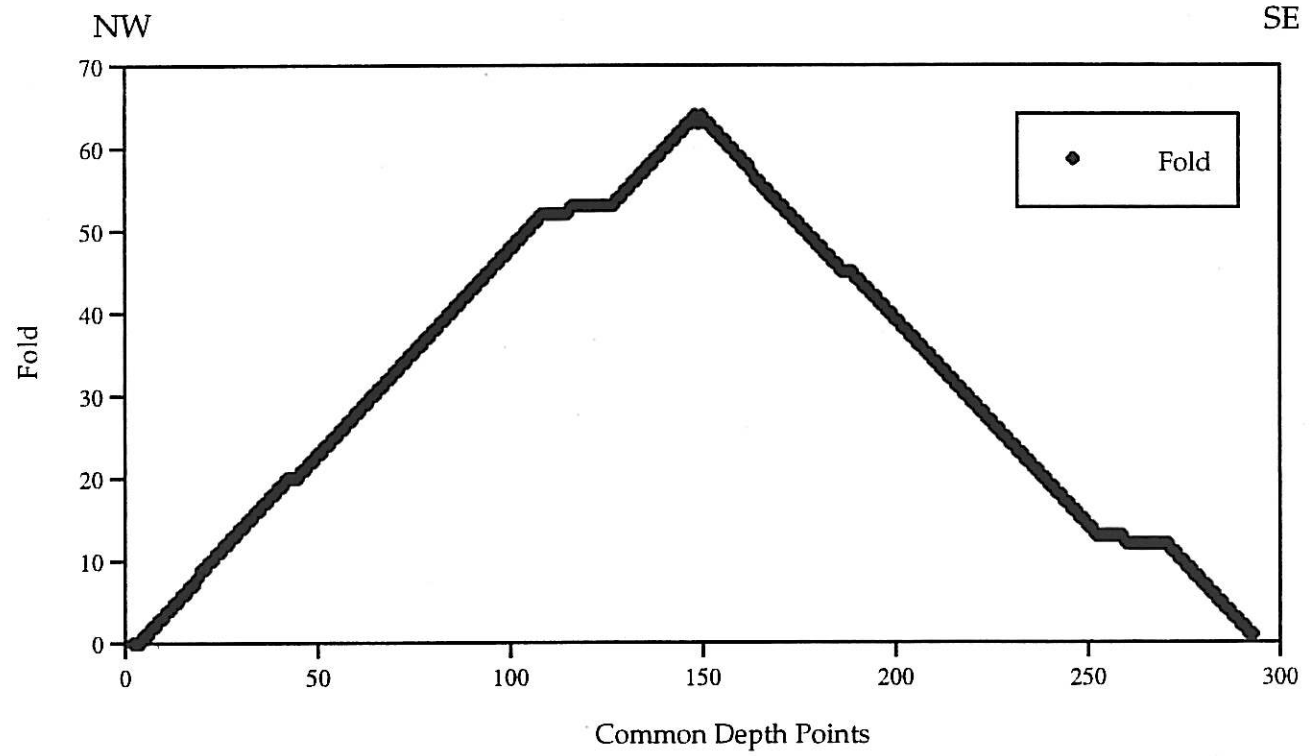

Figure 13: Fold as a function of common depth points (Line 2).

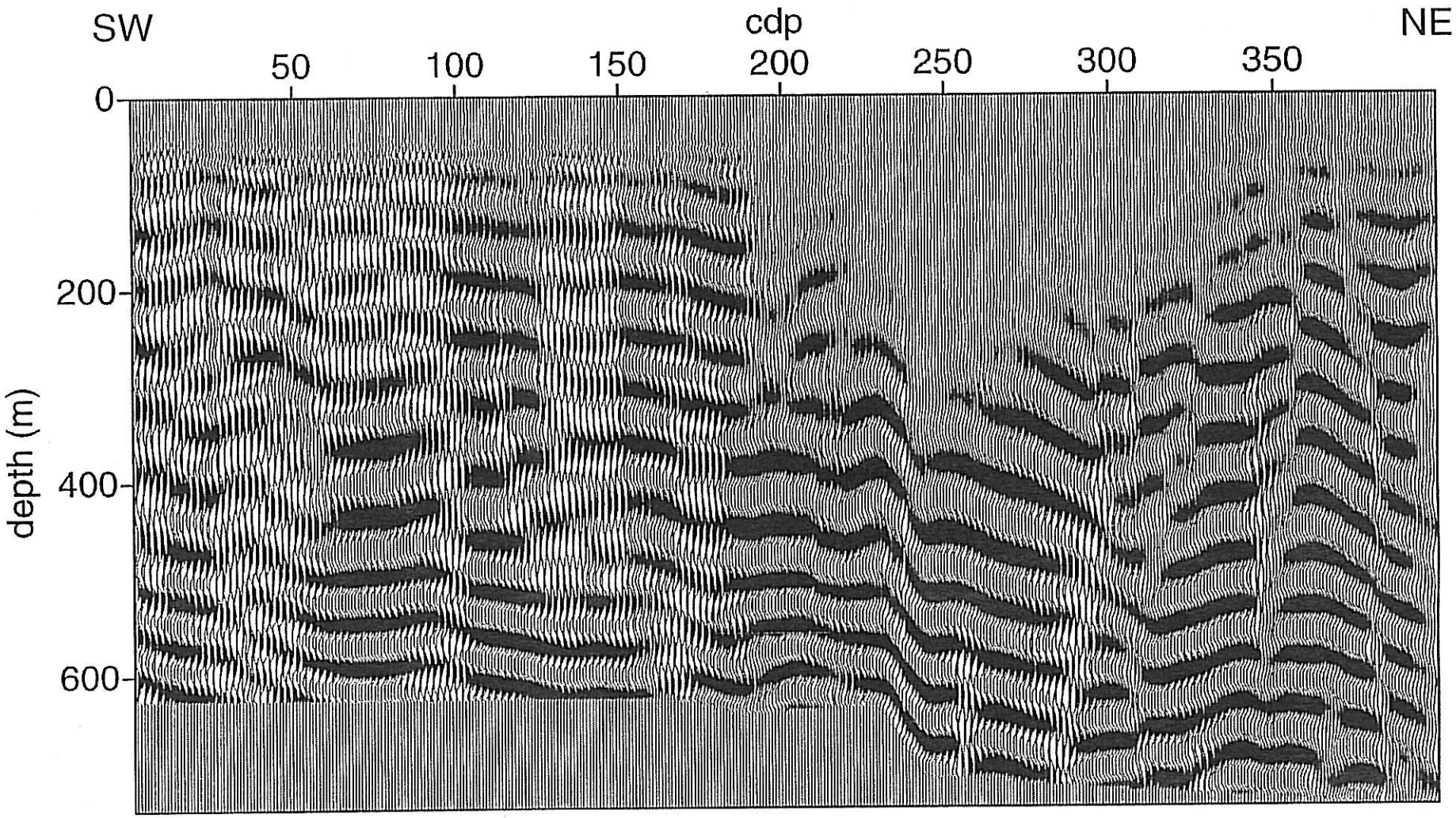

Figure 14: Stacked seismic section of Bottomless Pits - Line 1.

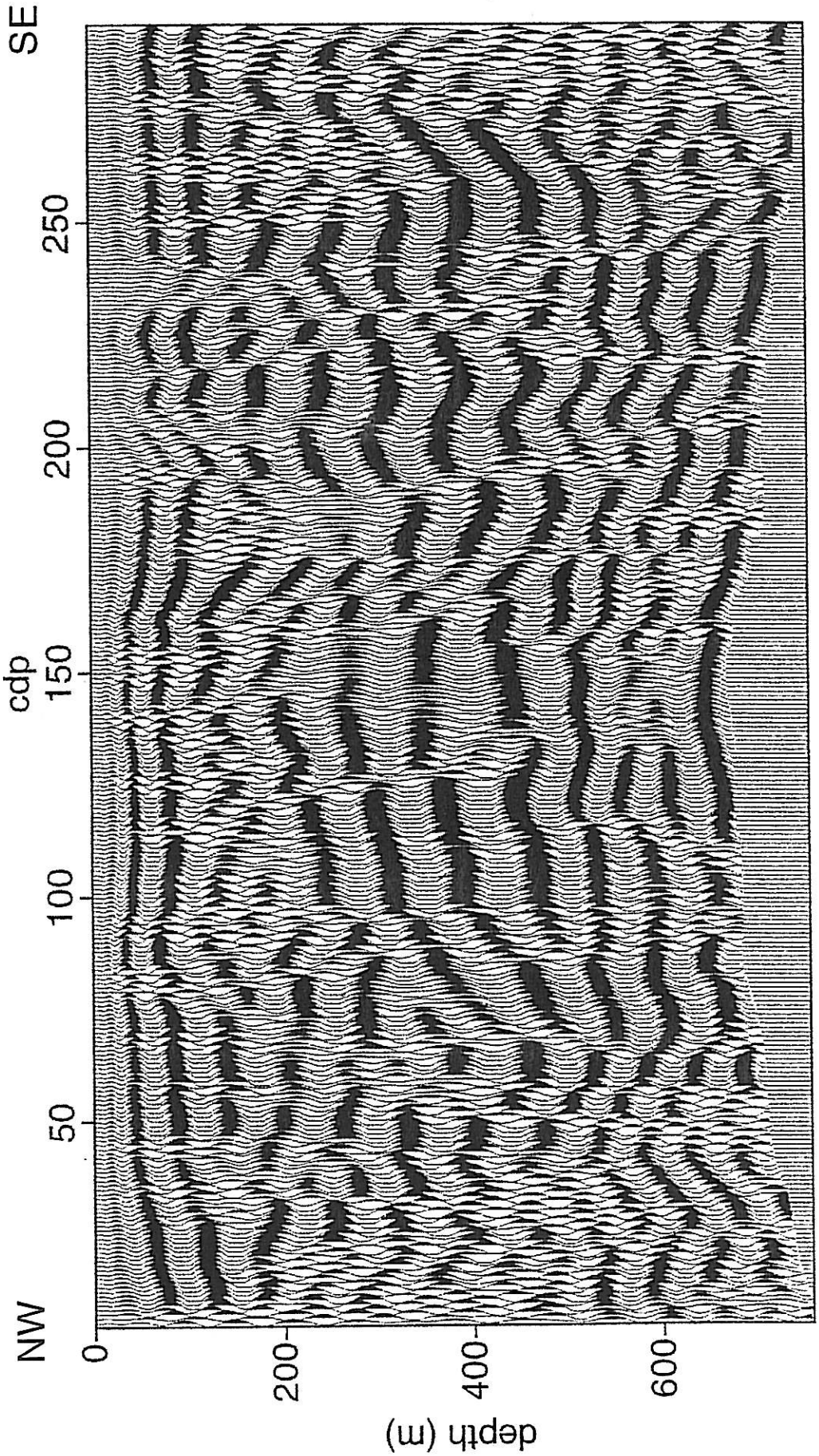

Figure 15: Stacked seismic section of Bottomless Pits - Line 2.

Acknowledgements

We thank Mike Abou-Ahmed, Sue Beard, Don Bills, Tom Burdette, Ed Criley, Cathy Cullicott, Christie O'Day, Herb Pierce, Sue Priest, Jose Rodriguez, Don Thorstenson, and volunteers from Northern Arizona University, the USGS-Flagstaff, and the USGS-Tucson for assistance in acquiring the seismic data. We thank A. Wesley Ward for providing funding and moral and logistical support. We thank Bob Hart for providing equipment and personnel, and Herb Pierce and Don Bills for providing geophysical and geological data. Ron Doba, Randy Pellatz, and Paul Peters provided invaluable logistical support. Funding was provided by the City of Flagstaff Water Commission and City Council. We thank Gary Mann for suggesting the locations of the seismic lines, providing targets for subsurface imaging, and providing many stimulating discussions. Discussions with George Billingsley are greatly appreciated. We thank Janice Murphy for reviewing.

References

Jaasma, M.N., R. D. Catchings, M. R. Goldman, and M. J. Rymer, 1997, Seismic Imaging Report for Eastern and Southern Flagstaff, Arizona, U.S. Geological Survey Open-file Report, 52 pp.

Mann, G., 1997, Fault and Fracture Map of Flagstaff, Arizona, Unpublished Map available through Northern Arizona University

Appendix A

Locations and elevations for Line 1. Distances and elevations are relative to the first receiver.

Shot Number	Receiver Dist. (m)	Receiver Elev. (m)	Shot Dist. (m)	Shot Elev. (m)
1	0.00	0.00	0.05	-0.08
	2.46	-0.04		
2	5.03	-0.06	5.12	-0.07
	7.47	-0.07		
3	10.01	-0.06	10.07	-0.06
	12.48	-0.07		
4	14.98	-0.05	15.07	-0.06
	17.49	-0.08		
5	20.03	-0.06	20.11	-0.08
	22.48	-0.08		
6	24.96	-0.09	24.99	-0.09
	27.45	-0.07		
7	29.91	-0.08	29.94	-0.06
	32.36	-0.08		
8	34.83	-0.03	34.93	-0.08
	37.32	-0.05		
9	39.81	-0.06	39.97	-0.09
	42.23	0.00		
10	44.69	0.03	45.17	-0.02
	47.19	-0.01		
11	49.67	-0.12	49.92	-0.15
	52.17	-0.04		
12	54.66	-0.09	55.01	-0.10
	57.13	-0.10		
13	59.65	-0.11	59.95	-0.15
	62.14	-0.12		
14	False	trigger		
15	64.65	0.01	64.95	-0.14
	67.15	-0.27		
	69.57	-0.13		
	72.04	0.14		
	74.54	0.31		
	77.05	-0.01		
16	79.55	-0.17	79.91	-0.23
	81.99	-0.20		
17	84.49	-0.19	84.96	-0.20
	86.98	-0.12		
	89.50	-0.04		
	91.85	-0.71		

Appendix A (cont.)

Shot Number	Receiver Dist. (m)	Receiver Elev. (m)	Shot Dist. (m)	Shot Elev. (m)
	94.42	-2.00		
	96.88	-0.75		
18	99.34	-0.51	99.84	-0.52
	101.81	-0.13		
19	104.33	-0.03	104.94	-0.05
	106.83	0.00		
20	109.32	0.00	109.95	-0.05
	111.87	0.02		
21	114.48	-0.01	114.75	-0.04
	116.95	0.01		
22	119.50	-0.01	119.96	-0.06
	122.00	-0.03		
23	124.56	0.02	124.82	0.00
24	False	trigger		
	127.11	0.01		
25	129.62	0.01	129.89	-0.02
	132.22	0.10		
26	134.65	0.14	134.72	0.08
	137.21	0.09		
27	139.74	0.09	139.82	0.04
	142.24	0.06		
	144.73	0.18		
	147.23	0.19		
28	149.79	0.00	149.93	0.03
	152.29	-0.06		
29	154.77	0.08	154.73	0.07
	157.30	0.03		
30	159.82	0.18	159.69	0.14
	162.37	0.19		
31	164.65	0.07	164.77	0.00
	167.32	0.05		
32	169.79	0.04	169.68	0.02
	172.30	0.11		
33	174.77	0.09	174.76	0.03
	177.27	-0.16		
34	179.84	-0.28	179.78	-0.29
	182.30	-0.33		
35	184.75	-0.28	184.66	-0.32
	187.28	-0.17		

Appendix A (cont.)

Shot Number	Receiver Dist. (m)	Receiver Elev. (m)	Shot Dist. (m)	Shot Elev. (m)
36	189.78	-0.04	189.70	-0.06
	192.28	0.05		
37	False	trigger		
38	194.78	0.11	194.64	0.09
	197.31	0.08		
39	199.84	0.00	199.69	-0.08
	202.32	-0.06		
	204.84	-1.37		
	207.30	-1.34		
40	209.81	-0.68	209.80	-0.75
	212.35	-0.92		
41	214.87	-1.12	214.80	-1.12
	217.45	-1.23		
42	False	trigger		
43	219.80	-1.19	219.81	-1.24
	222.33	-1.15		
44	224.81	-1.00	224.80	-1.07
	227.36	-0.99		
45	229.86	-0.72	229.80	-0.73
46	Off-line			
47	Off-line			
48	Off-line			
	232.30	-0.19		
	234.68	0.54		
	237.09	1.18		
	239.55	1.76		
	241.93	2.54		
	244.30	2.86		
	246.86	3.21		
	249.41	3.82		
	251.82	4.28		
	254.33	4.80		
	256.73	5.31		
	259.24	5.89		
	261.65	6.47		
	264.27	7.21		
	267.11	8.18		
	269.26	8.73		
	271.79	9.40		

Appendix A (cont.)

Shot Number	Receiver Dist. (m)	Receiver Elev. (m)	Shot Dist. (m)	Shot Elev. (m)
	274.24	9.86		
	276.68	10.39		
	279.30	11.03		
	281.63	11.55		
	284.03	12.01		
	286.43	12.80		
	288.82	13.67		
	291.21	14.59		
	293.59	15.50		
	296.04	16.24		
	298.47	17.02		
	301.02	17.90		
	303.71	18.76		
	305.77	19.26		
	308.41	19.93		
	310.72	20.45		
	313.16	20.99		
	315.81	21.64		
	318.04	22.18		
	320.58	22.71		
	323.08	23.36		
	325.71	23.79		
	327.96	24.20		
	330.69	24.74		
	335.60	25.61		
	338.11	25.99		
	340.57	26.46		
	342.97	26.84		
	345.42	27.33		
	347.90	28.00		
	350.29	28.52		
	352.75	28.86		
	355.16	29.10		
	357.59	29.26		
	360.12	29.40		
	362.44	29.55		
	364.81	29.67		
	367.22	29.81		
	369.58	30.00		

Appendix A (cont.)

Shot Number	Receiver Dist. (m)	Receiver Elev. (m)	Shot Dist. (m)	Shot Elev. (m)
	372.06	30.22		
	374.62	30.41		
	376.92	30.65		
	379.36	30.94		
	381.86	31.36		
	384.26	31.65		
	386.70	31.96		
	389.20	32.15		
	391.74	32.56		
	394.00	32.97		
	396.68	33.27		
	399.11	33.63		
	401.65	33.98		
	404.09	34.30		
	406.63	34.60		
	409.04	34.91		
	411.64	35.37		
	414.05	35.92		
	416.52	36.22		
	419.16	36.50		
	421.58	36.78		
	423.98	36.94		
	426.46	37.04		
	428.93	37.21		
	431.39	37.47		
	433.90	37.67		
	436.41	37.82		
	438.80	37.94		
	441.27	38.12		
49	443.80	38.40	443.98	38.44
	446.29	38.54		
50	448.75	38.65	449.46	38.59
	451.28	38.78		
51	453.89	38.95	454.42	38.83
	456.46	39.00		
52	458.99	39.06	459.39	38.95
	461.53	39.18		
53	False	trigger		
54	464.02	39.25	464.34	39.17

Appendix A (cont.)

Shot Number	Receiver Dist. (m)	Receiver Elev. (m)	Shot Dist. (m)	Shot Elev. (m)
	466.43	39.27		
55	468.86	39.36	469.41	39.30
	471.26	39.46		
56	473.81	39.56	474.30	39.48
	476.27	39.64		
57	478.74	39.70	479.37	39.65
	481.19	39.75		
58	483.77	39.88	484.20	39.86
	486.21	39.94		
59	488.75	40.04	489.44	40.09
	491.26	40.14		
60	493.81	40.22	494.34	40.20

Appendix B

Locations and elevations for Line 2. Distances and elevations are relative to the first receiver.

Shot Number	Receiver Dist. (m)	Receiver Elev. (m)	Shot Dist. (m)	Shot Elev. (m)
1	10.02	-0.04	10.02	-0.04
	12.50	0.00		
2	15.02	0.02	15.02	0.02
	17.59	0.07		
3	20.04	0.08	20.00	0.07
	22.53	0.09		
4	25.03	0.14	25.04	0.12
	27.53	0.09		
5	False	trigger		
6	29.97	0.08	29.99	0.07
	32.43	0.10		
7	34.94	0.12	35.01	0.08
	37.42	0.01		
8	39.93	0.04	40.00	0.02
	42.40	0.08		0.12
9	44.92	0.12	45.04	
10	49.92	0.03	50.01	0.02
	52.38	0.07		
11	54.94	0.14	55.01	0.13
	57.45	0.09		
12	59.87	0.06	60.10	0.06
	62.38	0.17		
13	64.91	0.14	65.03	0.11
	67.35	0.09		
14	69.81	0.10	70.02	0.04
	72.38	0.11		
15	74.94	0.13	75.14	0.14
	77.43	0.17		
16	79.98	0.24	80.06	0.19
	82.45	0.28		
17	84.90	0.00	85.15	0.02
	87.44	-0.15		
18	89.96	-0.51	90.13	-0.39
	92.37	-0.60		
19	94.91	-0.56	94.68	-0.54
	97.38	-0.16		
20	99.75	0.34	99.95	0.37
	102.42	0.60		
21	105.11	0.57	104.90	0.54

Appendix B (cont.)

Shot Number	Receiver Dist. (m)	Receiver Elev. (m)	Shot Dist. (m)	Shot Elev. (m)
	107.40	0.37		
	109.81	0.31		
	112.37	0.21		
22	115.01	0.14	114.97	0.14
	117.43	0.14		
23	119.98	0.11	119.85	0.11
	122.58	0.11		
24	125.06	0.13	124.84	0.11
	127.50	0.09		
25	129.93	0.09	129.81	0.02
	132.33	0.11		
26	134.76	0.12	134.90	0.10
	137.24	0.10		
27	139.66	0.14	139.92	0.03
	142.14	0.14		
28	144.59	0.17	144.96	0.15
	147.20	0.37		
29	149.74	0.17	149.95	0.17
	152.32	-0.09		
30	154.94	0.00	155.21	-0.05
	157.48	-0.01		
31	160.05	-0.05	160.19	-0.04
	162.61	-0.12		
32	165.10	-0.12	165.09	-0.12
	167.53	-0.11		
33	170.06	-0.05	170.17	-0.12
	172.49	0.00		
34	174.92	-0.01	174.97	0.01
	177.35	0.05		
35	179.90	0.07	180.10	0.04
	182.40	0.05		
36	185.00	0.03	185.14	0.00
	187.48	0.04		
37	190.05	0.03	190.16	-0.07
	192.56	0.06		
38	195.06	0.03	195.13	0.05
	197.60	0.09		
39	200.05	0.19	200.01	0.21
	202.53	0.22		

Appendix B (cont.)

Shot Number	Receiver Dist. (m)	Receiver Elev. (m)	Shot Dist. (m)	Shot Elev. (m)
40	205.03	0.03	205.03	-0.07
	207.51	-0.11		
41	210.03	-0.27	210.10	-0.34
	212.51	-0.23		
42	214.99	-0.29	215.01	-0.57
	217.46	-0.53		
43	219.97	-0.67	220.10	-0.72
	222.49	-0.67		
44	225.03	-0.65	225.11	-0.70
	227.52	-0.72		
45	229.94	-0.60	230.03	-0.59
	232.53	-0.58		
46	235.06	-0.51	235.02	-0.51
	237.58	-0.57		
47	239.92	-0.56	239.90	-0.65
	242.42	-0.58		
48	244.82	-0.61	244.92	-0.71
	247.36	-0.67		
49	249.93	-0.68	250.06	-0.69
	252.43	-0.64		
50	255.03	-0.68	255.21	-0.73
	257.59	-0.60		
51	260.10	-0.64	260.22	-0.65
	262.63	-0.62		
52	265.18	-0.62	265.06	-0.62
	267.76	-0.65		
53	270.18	-0.50	270.14	-0.51
	272.63	-0.42		
	275.24	-0.41		
	277.80	-0.40		
	280.41	-0.20		
	282.94	-0.18		
	285.51	-0.29		
	288.00	-0.40		
54	290.41	-0.31	290.13	-0.32
	292.97	-0.29		
	295.38	-0.25		
	297.82	-0.26		
	300.25	-0.14		

Appendix B (cont.)

Shot Number	Receiver Dist. (m)	Receiver Elev. (m)	Shot Dist. (m)	Shot Elev. (m)
	302.73	-0.14		
	305.04	-0.09		
	307.40	0.02		
	309.82	0.09		
	312.28	0.00		
	314.83	0.02		
	317.38	-0.07		
55	319.88	-0.12	319.96	-0.14
	322.33	-0.11		
56	324.81	0.03	324.87	-0.01
	327.25	-0.02		
57	329.75	0.00	329.84	0.01
	332.26	0.06		
58	334.73	0.12	334.95	0.03
	337.24	0.18		
59	339.72	0.03	339.96	0.03
	342.27	0.04		
60	344.86	0.06	344.99	0.05
	347.47	0.06		
61	350.07	0.08	350.16	0.01
	352.63	0.08		
62	355.13	0.06	355.22	0.04
	357.73	0.11		
63	360.24	0.08	360.19	0.07
	362.65	0.10		
64	365.35	0.08	365.28	0.08
	367.93	0.10		
65	370.25	0.14	370.05	0.13
	372.71	0.17		
66	False	trigger		
67	False	trigger		
68	375.17	0.18	375.16	0.16
	377.58	0.03		